Monte Carlo uncertainty analysis of an ANN based spectral analysis method

J.R. Salinas[1], F. García-Lagos[1], J. Díaz de Aguilar[2], G. Joya[1] and F. Sandoval[1]

[1] Grupo ISIS, Dpto. Tecnología Electrónica, ETSI Telecomunicación, Universidad de Málaga

Campus de Teatinos s/n, 29071 Málaga, Spain

jrsalinas@uma.es

[2] Centro Español de Metrología (CEM)

Alfar 2, 28760 Tres Cantos, Spain

Abstract This work presents the uncertainty analysis of an Artificial Neural Network (ANN) based method, called Multiharmonic ANN fitting method (MANNFM), which is able to obtain, at a metrological level, the spectrum of asynchronously sampled periodical signals. For sinusoidal and harmonic content signals, jitter and quantization noise contributions to uncertainty are considered in order to obtain amplitude and phase uncertainties using Monte Carlo method. The analysis performed identifies also both contributions to uncertainty for different parameters laboratory configurations. The analysis is performed simultaneously with our method and two others: Discrete Fourier Transform (DFT), for synchronously sampled signals, and Multiharmonic Sine Fitting Method (MSFM), for asynchronously sampled signals, in order to compare them in terms of uncertainty. Regarding asynchronous methods, results show that MANNFM provide the same uncertainties than MSFM, with the advantage of a simpler implementation. Regarding asynchronous and synchronous methods comparison, results for sinusoidal signals show that MANNFM has the same uncertainty as DFT for amplitude and higher uncertainty for phase values; for signals with harmonic content, amplitude conclusions maintain but, regarding phase, both MANNFM and DFT uncertainties become closer as the frequency increases, which implies, in fact, that when synchronous sampling is not possible, spectrum analysis can be performed with asynchronous methods without incurring in uncertainty increases.

Keywords: sine-fitting methods; spectral analysis; ADALINE; digital measurement; uncertainty; Monte-Carlo.

adfa, p. 1, 2011.

1 Introduction

The use of nonlinear electronic components connected to the electrical grid is becoming common in our daily life. These components add harmonic and inter-harmonic content to the electric signal, which results in a deterioration of the quality of the power supplied, an increase in losses and a decrease in the reliability of the whole system. In this situation, it is increasingly important to accurately determine the harmonic content of the power signals. For these reasons, several National Metrological Institutes (NMIs) have implemented new methods to measure power in non-sinusoidal conditions [1] [2].

These new methods make use of the versatility of the digital techniques, especially considering the possibility of obtaining the spectral analysis of the signals of interest, and are based on the use of traditional algorithms, such as DFT. In order to be accurate, DFT requires synchronous sampling [3], which, in real measurement systems, implies that sampling and generation time bases must be common, which is not always possible. If this condition cannot be accomplished, the DFT spectral analysis of the sampled signals incurs in errors due to the spectral leakage effect.

To overcome this limitation, some authors [4] [5] have proposed the use of asynchronous sampling combined with the use of non-synchronous spectral analysis methods. In particular, sine fitting methods [6] have been successfully extended to the multi-harmonic case [4] [5] [7] as a way to perform spectral analysis of asynchronously sampled signals without incurring in spectral leakage errors (and with the resultant simplification of the real measurement systems).

Alternatively, a new method based on ANN was presented in [8]. This last is based on the implementation of the multi-harmonic sine fitting algorithm [6] by mean of a multilayer perceptron neural network (MLP). The ANN method, called MANNFM, as the sine fitting, has the advantage with respect to the traditional spectral analysis methods that it does not require synchronism between generation and sampling, which reduce the complexity of the hardware implementation. In comparison with the conventional multi-harmonic sine fitting method, the ANN method has a simpler implementation and does not require special adjustments of coefficients for convergence, which depend on the type of signal being analysed [7]. The proposed method has been implemented in the Spanish electrical power primary standard, at the Spanish National Metrology institute (CEM for its Spanish acronym) [9] [10]. Additionally, this approach has the advantage of allowing, with reduced complexity, modifications of the signal model to be analysed. In this sense, this method was recently extended to obtain inter-harmonic components in [11].

At a metrological primary level, the traceability of such a sampling system is a complex task due to the complexity of the tests and validations of involved algorithms. Thus, the main contribution of the present work is the validation and uncertainty evaluation, for both sinusoidal signals and harmonic content signals, of the ANN-based spectral analysis method proposed in [8] by means of Monte Carlo

method. In order to obtain useful results for real applications, we have considered parameter configurations frequently used in normal calibrations.

The present paper is an extension of [12], which only considered sinusoidal signals (but not harmonic content signals). In order to make this work self-contained, descriptions of the proposed method and the methodology applied in the study are included in this document. With respect to sinusoidal signals results, this work will only present the obtained conclusions. The reader is invited to consult detailed results in [12].

Thus, this article is structured as follows: in section 2, the system to be characterized is briefly presented; in section 3, the Monte Carlo method applied to the characterization of high precision measurement systems is introduced; the test methodology is described in section 4; results for sinusoidal signals are summarized in section 5; results for signals with harmonic content are reported in section 6; and, finally, section 7 exposes the conclusions of this work.

2 Network description

Let us consider a signal of interest, $y(t)$, (t considered to be continuous), composed of K harmonic frequencies of the fundamental frequency, f_{ac}. Let us also considered that, during the time interval of analysis, the possible variations of the signal's parameters are bounded to known and small values, so that these variations can be neglected. The signal $y(t)$ can be described mathematically, eq. (1), as a DC component, C, added to the combination of phase (cosines) and quadrature (sines) terms for the different frequencies $f_k=k \bullet f_{ac}$, $k \in [1, K]$ -being k=1 the fundamental frequency.

$$y(t) = C + \sum_{k=1}^{K} [A_k \cdot \cos(2\pi k f_{ac} t) + B_k \cdot \sin(2\pi k f_{ac} t)] \quad (1)$$

The proposed ANN-based method [8], MANNFM (Multiharmonic ANN Fitting Method), performs the spectral analysis of a steady state periodical signal as described in equation (1). This is done by means of the multilayer neural network of Figure 1.

Input data to the ANN are the N time instants - $t[n]$, $n \in [0, N\text{-}1]$- at which the samples of $y(t)$, $y[n]$, are taken. The time vector, t, is scaled by the factor $2 \cdot \pi$ in order to generate the arguments of cosines and sines of eq. (1).

The network implements the K order Fourier series synthesis equation. Briefly, Layer 1, implemented by means of an ADALINE neuron without bias and linear transfer function, has the object of implementing the scale factor of the fundamental frequency, f_{ac}, in the arguments of the cosines and sines of the synthesis equation. The output of Layer 1 is connected in parallel to Layers 2 and 3, both of which are implemented by K ADALINE neurons with cosine and sine transfer functions, respectively. The position of each neuron in the array of neurons determines its weight value, so that the k scale factor of each harmonic in the cosine

and sine arguments is implemented by this weight. As a result, the input to the transfer functions of the neurons of Layers 2 and 3 are the completed arguments of the cosines and sines of the Fourier synthesis equation.

Consequently, the inputs from the harmonic section to Layer *4* are the arrays $cos(2\cdot\pi\cdot k\cdot f_{ac}\cdot t)$, $k\in [1, K]$ and $sin(2\cdot\pi\cdot k\cdot f_{ac}\cdot t)$, $k\in [1, K]$. Finally, Layer *4* implements the summatory in the synthesis equation, by means of $2\cdot K$ neurons with linear transfer functions. The weights of the neurons connected to Layer *2* are identified as the A_k coefficients of eq. (1), and the weights of the neurons connected to Layer *3* are identified as the B_k coefficients of eq. (1). In addition, Layer *4* includes the DC component of the Fourier synthesis series, C, by means of its bias value, which is available in this layer. Therefore, at this point, Layer *4* output is equivalent to the output of the eq. (1), $y(t)$, in the time instants $t[n]$, $n\in[0, N-1]$.

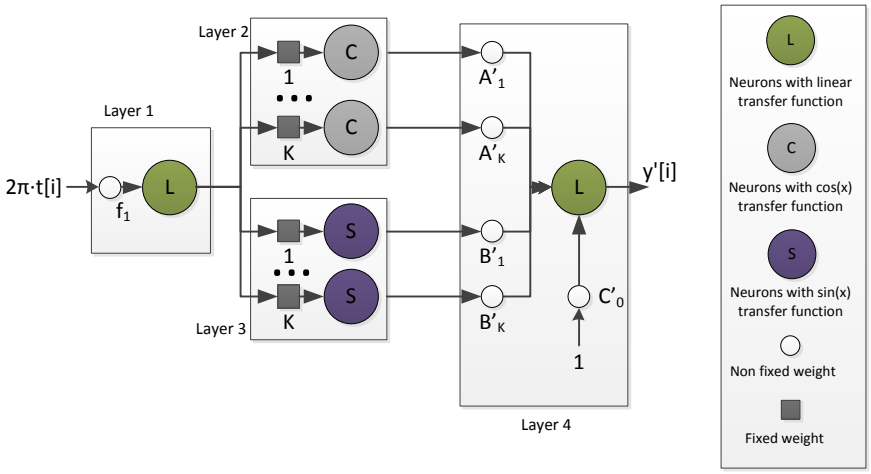

Fig. 1. Proposed ANN architecture [8].

As mentioned above, this high precision algorithm has been implemented and tested in the measurements system of the CEM as part of the electrical power primary standard.

3 Propagation of distributions and its simulation using the Monte Carlo method

The Guide to the Expression of Uncertainty in Measurement (GUM) [13] provides the framework for uncertainty evaluation, which has three main stages: formulation, propagation and summarizing. At the *Formulation* stage the N input quantities, $\boldsymbol{I} = (I_1, \ldots, I_N)$ upon which the output quantity, O, depends, are determined, and their probability distribution functions (PDF), are assigned. In the *Propagation* stage, the PDFs for the I_i are propagated through the measurement

model, $O = f(\boldsymbol{I})$, in order to obtain the PDF of the output O. Finally, in the *Summarizing* stage, using the PDF obtained for O, the expectation of O, o, and its standard deviation, $u(o)$, are obtained.

The propagation of distributions can be implemented analytically (by mathematical representations or approximated models) or by numerical methods particularly by MCM [14]. As mentioned previously, due to the complexity of the MANNFM uncertainty evaluation, the Monte-Carlo method (MCM) will be used.

The basis of MCM, Figure 2, is to reconstruct the PDF for O, obtaining M values o_r, for $r = 1, \ldots, M$. If the input quantities are independent, as they are in this work, each o_r is obtained by sampling at random from each one of the PDFs for I_i and evaluating the model at the samples values so obtained. In case of several output variables [15], the foundation is the same but $\boldsymbol{O}$ is a vector provided by a vector function or model $\boldsymbol{f(O)}$.

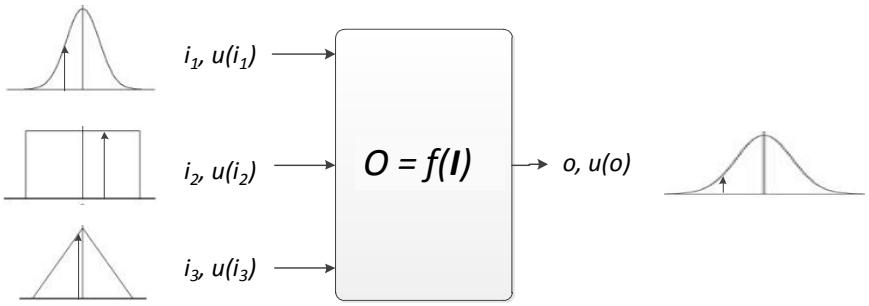

Fig. 2. MCM propagation of distributions for 3 independent input quantities

Although Monte Carlo method is used as a mean to provide a numerical representation of the PDF for O, it is also a simulation process that provides information about the input/output PDFs relationship of a system modelled as $f(O)$. So, the method can be used not only to obtain output uncertainties of a measurement, but also to simulate a system [16] and evaluate the impact of different parameters as well as the impact of the different uncertainty contributions on the output uncertainties. The second approach will be used in this work.

4 Methodology

4.1 Simultaneous methods comparison

In order to compare MANNFM results with those obtained by other methods, the same tests have been applied to other two methods: DFT [3] and MSFM [7].

DFT can be considered as a reference, given that, in ideal conditions, provides the spectrum of the signal under analysis without error. When synchronous sampling is not possible, fitting methods are used [4] [6] in order to avoid DFT errors due to spectral leakage. For comparison purposes the same signal, $x(t)$, will be sampled and applied to the three methods as shown in Figure 3. The DFT will process synchronous samples of $x(t)$, $x_s[n]$, while MSFM and MANNFM will process asynchronous samples of $x(t)$, $x_a[n]$, obtained in a set of time instants $t_a[n]$, where $t_a[n]=t[n]\cdot(1+\xi_a)$, being ξ_a the error of synchronism (relative) between generation and sampling[1]. Regarding the Monte Carlo method described in section 3: methods will be the relationship, f; time instants and samples applied will be the input, $\boldsymbol{I}$; and spectrum obtained will be the output, O.

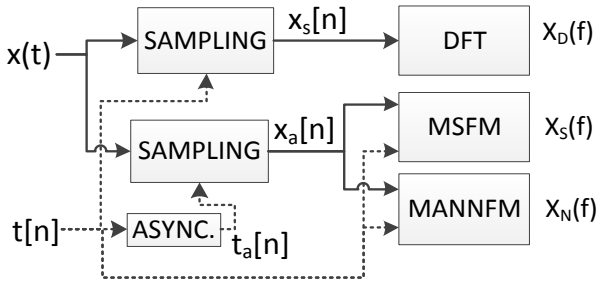

Fig. 3. Scheme for the comparison of the three methods

4.2 Uncertainties contributions considered

For the uncertainty evaluation, two main uncertainty components will be considered in this work: jitter influence to the time of each sampled point (the sampling jitter); and quantization contributing to the voltage of each sampled point. Both of them have been theoretically studied for DFT [17] [18]. Obviously, quantization and jitter are independent variables (one is the effect of the limited number of codes of the analog to digital converter while the other is due to reasons as noise on the sampling impulse signal, clock instability, etc), consequently, as it was mentioned in section 3, independent sampling of both inputs distributions will be performed. Regarding jitter, a rectangular distribution has been considered.

[1] The error of synchronism is due to the differences between generation and sampling time bases. Authors expertise (with real and simulated signals) have shown that this error affects only to the convergence of the method to global or local minima, but not to the value of these minima. So, it will not be considered an uncertainty source. Nevertheless, it has been included in simulations just to perform the uncertainty evaluation in the more general conditions.

Taking into account the specifications of usual laboratory instruments[2], two jitter values will be contemplated: $3 \cdot 10^{-12}$ s and $1 \cdot 10^{-7}$ s. The first value is the jitter specification for the National Instruments 5922 digitizer, and the second one is the jitter specifications for the Keysight 3458A digital multimeter used in [9] [10]. So, two different rectangular distributions with interval limits of $\pm 1.5 \cdot 10^{-12}$ s and $\pm 0.5 \cdot 10^{-7}$ s will be used.

Concerning the quantization, it has been simulated taken into account three usual laboratory resolutions or number of bits, *Nbits,* values: 16, 18 and 21 bits, which correspond with 3458A and NI 5922 resolution values derived from high, medium and low sampling frequencies, respectively (NI 5922 can provide higher resolution values, not considered in this work). Regarding the range, *R*, 1.2 V has been used, which is the full-scale value for the 1 V range of the 3458A in digital operation mode. With these parameters [1], the maximum error due to quantization, ε_{Qmax}, could be calculated as $\varepsilon_{Qmax} = 2 \cdot R/2^{Nbits}$. This error distribution can be considered uniformly distributed between its limits. So, three different rectangular distributions with interval limits of $\pm 1.83 \cdot 10^{-5}$ V, $\pm 4.58 \cdot 10^{-6}$ V and $\pm 5.72 \cdot 10^{-7}$ V will be used.

In order to carry out both an independent and joint evaluation of the impact of both contributions to the combined uncertainty for the three methods, the scheme presented in Figure 3 will be simulated with three different sampling situations: (i) samples only affected by quantization; (ii) samples only affected by jitter; and (iii) samples affected by quantization and jitter. Terms *q, j* and *jq*, respectively, will be used in reference to signals and results related to these three sampling situations.

4.3 Parameter values

Several parameters values of the signal to be sampled (those corresponding to the most useful for the laboratory calibration work), have been considered in order to evaluate their impact on the estimated uncertainty.

Regarding the ratio $R=f_s/f_{ac,}$ being f_{ac} the fundamental frequency and f_s the sampling frequency, three values have been selected, around 24, 123 and 262, related to low, medium and high sampling frequencies, respectively.

Concerning the number of samples, *N*, and the number of periods involved in the measurement *M*, it has to be considered that (i) the maximum capacity of the Keysight 3458 internal memory (for maximum precision), is 37888 samples, and (ii) *N* and *M* should not have common factors in order to obtain maximum information of the sampled signal. Consequently, three *N* values (1311, 7073 and 15457), related to low, medium and high number of samples have been selected and used in each ratio value. *R* can also be expressed as $R=N/M$. So, variations of *N* keeping *R* constant implies also to vary *M*. Table 1 shows the values of *R*, *N* and

[2] Brand names are used for purpose of identification. Such use does not imply endorsement by authors or assume that the equipment is the best available.

M considered. In order to assure the DFT conditions, *N* and *M* integer values have been selected (which imply light variations of the obtained ratio *R*).

N		M	R	fs
H	15457	59	261.983	
M	7073	27	261.963	H
L	1311	5	262.200	
H	15457	125	123.656	
M	7073	57	124.088	M
L	1311	11	119.182	
H	15457	625	24.731	
M	7073	286	24.731	L
L	1311	53	24.736	

Table 1. Sampling frequency parameters values considered to estimate the uncertainty of the system. H, M, L represents High, Medium and Low, respectively

Finally, in relation to the error of synchronism, ξ_a, random values up to *±20%,* uniformly distributed, have been considered. In order to obtain initial estimation of the fundamental frequency for the asynchronous methods, the Interpolated FFT (*IpFFT*) [19] algorithm has been used. No convergence problems have been detected in any simulation.

4.4 Processing procedure

All tests have been performed with the selected parameters and the uncertainty contributions defined in previous sections. 10^6 trials of the MCM have been simulated over the three methods in order to obtain a numerical representation of their PDF outputs.

All the obtained PDFs are Gaussian. The values have been expressed in deviations to nominal and those deviations have been fitted to a Normal PDFs by means of Matlab© *normfit* function, obtaining their mean, *E*, (as deviation to nominal) and the standard deviation, σ. In next subsections the most significant results of the tests performed, in terms of mean and standard deviation, will be presented.

4.5 Computational hardware

In order to perform 10^6 trials of the MCM over the three methods in the different established configurations, large computational resources are required. For this work, resources provided by the University of Málaga‘s Supercomputing Centre (UMSC) have been used. These computational resources are based on the Cluster Intel E5-2670, with shared memory machines with 2 TB of RAM, AMD Opteron 6176 and ESX virtualization clusters.

5 Results for sinusoidal signals

Detailed information about results for sinusoidal signals can be found in [12]. Here we will present just the conclusions of this work.

First of all, for all different parameter configuration simulated, it was found that the mean of deviations to nominal for amplitude and phase were around zero, with values always lower than $2 \cdot 10^{-3}$ μV and $2 \cdot 10^{-3}$ μrad, respectively.

Besides, results also showed that the jointly impact of jitter and quantization was equivalent to the quadratic sum of the independent impacts as expected, since both effects were generated independently.

Concerning method comparison, the results of both fitting methods were almost identical in all different simulations (which is logical, due both methods solve the same optimization problem in a different way). Comparing DFT and fitting methods, both provided practically identical standard deviation in amplitude, but higher (in a factor around 2) was obtained in phase standard deviation by fitting methods.

About R and N, their effect was the same for the three methods: it was found that R value does not affect the standard deviations of amplitude and phase, while the N value impacts clearly in the results, so that lower N values produce higher standard deviations.

Finally, concerning the combined effect of jitter and number of bits in methods results, it was concluded that for a jitter value of 3 ps, the combined contribution to the combined uncertainty could be approximated by the quantization contribution. Nevertheless, for 100 ns of jitter, it was shown that quantization effect could be discarded for 21 bits, while for 18 bits both effects had similar contribution and for 16 bit, the jitter effect could be discarded.

6 Results for signals with harmonic content

For the uncertainty study with harmonic content, two signals were considered: a sinusoidal half-wave rectified (*HWR*) signal up to the 10th harmonic, and a triangular (*TRI*) signal up to the 11th harmonic. The half-wave rectified signal was selected due to its use in laboratory tests for energy meters [20]. On the other hand, triangular signal is frequently used in harmonic studies and has a similar spectra distribution but in odd harmonics. Hence, for all simulations, input signal, $x(t)$, was modelled according to eq. (2). Fundamental frequency, f_{ac}, was fixed to 53 Hz. Tables 2 and 3 presents amplitudes, A_k, and phases, ϕ_k, for *HWR* and *TRI* signals, respectively. For both cases, fundamental phase, ϕ_1, was generated as a random number with rectangular probability between $\pm\pi$ radians and harmonic phases were calculated appropriately for each harmonic.

$$y(t) = C + \sum_{k=1}^{K} A_k \cdot \cos(2\pi k f_{ac} t + \phi_k) \quad (2)$$

k	A_k	Φ_k
0	0.318 309 9	- -
1	0.500 000 0	-π/2
2	0.212 206 6	-π
4	0.042 441 3	-π
6	0.018 189 1	-π
8	0.010 105 1	-π
10	0.006 430 5	-π

Table 2. Harmonics amplitudes (V) and phases (radians) according to eq. (2) for half-wave rectified signal considering peak value of 1V and ϕ_1=0 rad

k	A_k	Φ_k
1	0.810 569 5	-π/2
3	0.090 063 3	π/2
5	0.032 422 8	-π/2
7	0.016 542 2	π/2
9	0.010 007 0	-π/2
11	0.006 698 9	π/2

Table 3. Harmonics amplitudes (V) and phases (radians) according to eq. (2) for triangular signal, considering peak value of 1 V and ϕ_1=0 rad

6.1 Method comparison

The same tests performed for method comparison in sinusoidal conditions (*Maxjitt* =100 ns, *Nbits* = 16, *N*=15457 and *M*=625) were carried out with *HWR* and *TRI* signals. First, results obtained for fundamental frequency will be presented. After that, results for harmonics will be exposed.

6.1.1 Fundamental frequency

For both signals, Tables 4, 5 and 6 show the results considering the impact on the three methods of only jitter, only quantization and the combination of both contributions, respectively. Tables show the standard deviations to nominal for both amplitude and phase of the fundamental frequency component. For amplitude, standard deviations are presented as relative values (to nominal amplitude, A_{1_n}), in order to be able to compare results of different signals amplitudes.

	Half wave rectified fundamental				Triangular fundamental			
	$E_j\{\Delta A_1\}$ (μV)	$\sigma_j(\Delta A_1)$ / A_{1_n} (μV/V)	$E_j\{\Delta\Phi_1\}$ (μrad)	$\sigma_j(\Delta\Phi_1)$ (μrad)	$E_j\{\Delta A_1\}$ (μV)	$\sigma_j(\Delta A_1)$ / A_{1_n} (μV/V)	$E_j\{\Delta\Phi_1\}$ (μrad)	$\sigma_j(\Delta\Phi_1)$ (μrad)
DFT	-2.70E-04	7.72E-02	-5.40E-04	1.31E-01	-1.10E-04	8.50E-02	-2.60E-04	8.49E-02
MPSF	-4.90E-04	7.88E-02	-4.20E-03	2.65E-01	-2.00E-04	8.44E-02	1.20E-04	1.62E-01
MANNFM	-4.90E-04	7.88E-02	-4.20E-03	2.65E-01	-2.00E-04	8.44E-02	1.20E-04	1.62E-01

Table 4. Mean (E) and standard deviation (σ) of the fundamental frequency component as deviations to nominal amplitude (relative) and phase for the three methods - only jitter considered

	Half wave rectified fundamental				Triangular fundamental			
	$E_q\{\Delta A_1\}$ (μV)	$\sigma_q(\Delta A_1)$ / A_{1_n} (μV/V)	$E_q\{\Delta\Phi_1\}$ (μrad)	$\sigma_q(\Delta\Phi_1)$ (μrad)	$E_q\{\Delta A_1\}$ (μV)	$\sigma_q(\Delta A_1)$ / A_{1_n} (μV/V)	$E_q\{\Delta\Phi_1\}$ (μrad)	$\sigma_q(\Delta\Phi_1)$ (μrad)
DFT	1.60E-04	2.46E-01	3.70E-04	2.36E-01	1.60E-04	1.48E-01	2.90E-04	1.50E-01
MPSF	-1.20E-04	2.43E-01	-3.60E-04	3.84E-01	2.30E-04	1.50E-01	1.30E-04	2.84E-01
MANNFM	-1.20E-04	2.43E-01	-3.60E-04	3.84E-01	2.30E-04	1.50E-01	1.30E-04	2.84E-01

Table 5. Mean (E) and standard deviation (σ) of the fundamental frequency component as deviations to nominal amplitude (relative) and phase for the three methods - only quantization considered

	Half wave rectified fundamental				Triangular fundamental			
	$E_{jq}\{\Delta A_1\}$ (μV)	$\sigma_{jq}(\Delta A_1)$ / A_{1_n} (μV/V)	$E_{jq}\{\Delta\Phi_1\}$ (μrad)	$\sigma_{jq}(\Delta\Phi_1)$ (μrad)	$E_{jq}\{\Delta A_1\}$ (μV)	$\sigma_{jq}(\Delta A_1)$ / A_{1_n} (μV/V)	$E_{jq}\{\Delta\Phi_1\}$ (μrad)	$\sigma_{jq}(\Delta\Phi_1)$ (μrad)
DFT	-1.10E-03	2.58E-01	3.70E-02	2.69E-01	5.00E-04	1.70E-01	3.30E-04	1.73E-01
MPSF	-1.70E-02	2.55E-01	-7.80E-02	4.74E-01	2.10E-03	1.71E-01	1.40E-02	3.28E-01
MANNFM	-1.70E-02	2.55E-01	-7.80E-02	4.74E-01	2.10E-03	1.71E-01	1.40E-02	3.28E-01

Table 6. Mean (E) and standard deviation (σ) of the fundamental frequency component as deviations to nominal amplitude (relative) and phase for the three methods - jitter and quantization considered

All conclusions obtained in the comparison for sinusoidal signals can be applied to the fundamental frequency with harmonic content signals: in all cases mean of deviations to nominal are around zero; fitting methods provides almost identical results; DFT and fitting methods standard deviations are quite similar in amplitude but DFT phase values are slightly better; for the parameters configured, standard deviation obtained considering only quantization are higher than those obtained considering only jitter; and combined effect of jitter and quantization is equivalent to the quadratic sum of the independent contributions.

In addition, comparing harmonic and sinusoidal results, other considerations can be established. Firstly, the standard deviations obtained (in amplitude and phase) for fundamental frequency in harmonic cases are in the same range as in the sinusoidal case. For example, for sinusoidal, half-wave rectified and triangular signals, amplitude standard deviations considering only jitter contribution to uncertainty are in the order of 10^{-2} μV while results considering only quantization contribution are in 10^{-1} μV. Secondly, although in the same range, results are slightly different depending on the signal spectral content. Thus, for example, while quantization provokes around $2.5 \cdot 10^{-1}$ μV/V in half-wave rectified signal, for triangular signal this value is around $1.5 \cdot 10^{-1}$ μV/V and was $1.1 \cdot 10^{-1}$ μV/V for the sinusoidal case. Similar considerations can be done regarding phase results.

6.1.2 Harmonic frequencies

Tables 7 and 8, for *TRI* and *HWR* signals respectively, show, for each harmonic, the standard deviations of deviations to nominal values for both amplitude (relative) and phase. Due to space limitations, mean values (also near to zero, as shown in previous section for fundamental frequency component) will not be presented for harmonics. Similarly, given that fitting methods provide effectively identical results, only MANNFM results will be presented from now on.

As for sinusoidal signal, results show again that: mean deviations are around zero; fitting methods provides identical results; DFT and fitting methods results are similar in amplitude; DFT phase results are slightly lower than fitting methods; and combined effect of jitter and quantization is equivalent to the quadratic sum of their independent effects. Considering last point, from now on, combined jitter and quantization results will not be presented.

		DFT			MANNFM		
	Harm	j	q	jq	j	q	jq
$\sigma(\Delta A_i)/A_{i\_n}$ (μV/V)	1	8.50E-02	1.48E-01	1.70E-01	8.44E-02	1.50E-01	1.71E-01
	3	7.48E-01	1.32E+00	1.51E+00	7.52E-01	1.37E+00	1.58E+00
	5	2.02E+00	3.76E+00	4.20E+00	2.08E+00	3.67E+00	4.22E+00
	7	3.98E+00	7.32E+00	8.34E+00	4.08E+00	7.22E+00	8.24E+00
	9	6.64E+00	1.19E+01	1.38E+01	6.76E+00	1.18E+01	1.36E+01
	11	1.01E+01	1.79E+01	2.08E+01	1.03E+01	1.76E+01	2.02E+01
$\sigma(\Delta\Phi_i)$ (μrad)	1	8.49E-02	1.50E-01	1.73E-01	1.62E-01	2.84E-01	3.28E-01
	3	7.61E-01	1.31E+00	1.50E+00	8.88E-01	1.49E+00	1.74E+00
	5	2.22E+00	3.74E+00	4.33E+00	2.36E+00	3.92E+00	4.62E+00
	7	4.14E+00	7.18E+00	8.18E+00	4.31E+00	7.54E+00	8.71E+00
	9	6.96E+00	1.18E+01	1.38E+01	6.88E+00	1.20E+01	1.39E+01
	11	1.03E+01	1.77E+01	2.09E+01	1.05E+01	1.85E+01	2.12E+01

Table 7. Triangular signals. Standard deviations of the deviations to nominal values for amplitude (μV/V) and phase (μrad), considering: only jitter (*j*), only quantization (*q*) and both (*jq*)

		DFT			MANNFM		
	Harm	j	q	jq	j	q	jq
$\sigma(\Delta A_i)/A_{i\_n}$ (μV/V)	0	1.19E-01	2.65E-01	2.92E-01	1.21E-01	2.65E-01	2.90E-01
	1	7.72E-02	2.46E-01	2.58E-01	7.88E-02	2.43E-01	2.55E-01
	2	2.45E-01	5.59E-01	6.03E-01	2.51E-01	5.62E-01	6.17E-01
	4	1.23E+00	2.84E+00	3.13E+00	1.24E+00	2.90E+00	3.15E+00
	6	2.79E+00	6.66E+00	7.25E+00	2.80E+00	6.43E+00	7.09E+00
	8	5.24E+00	1.17E+01	1.26E+01	5.26E+00	1.20E+01	1.29E+01
	10	8.23E+00	1.87E+01	2.07E+01	8.63E+00	1.86E+01	2.06E+01
$\sigma(\Delta\Phi_i)$ (μrad)	0	--	--	--	--	--	--
	1	1.31E-01	2.36E-01	2.69E-01	2.65E-01	3.84E-01	4.74E-01
	2	2.59E-01	5.65E-01	6.20E-01	5.28E-01	8.29E-01	9.81E-01
	4	1.31E+00	2.85E+00	3.14E+00	1.61E+00	3.08E+00	3.49E+00
	6	3.08E+00	6.69E+00	7.30E+00	3.40E+00	6.89E+00	7.71E+00
	8	5.42E+00	1.22E+01	1.34E+01	5.75E+00	1.22E+01	1.35E+01
	10	8.36E+00	1.83E+01	2.03E+01	8.80E+00	1.90E+01	2.09E+01

Table 8. Half wave rectified signals. Standard deviations of the deviations to nominal values for amplitude (μV/V) and phase (μrad), considering: only jitter (*j*), only quantization (*q*) and both (*jq*)

Regarding frequency dependence, Fig. 4 shows standard deviations of amplitude and phase deviations to the nominal values for both *HWR* and *TRI* signals considering only quantization (similar figures are obtained for jitter and combined effects). It can be observed that: 1) in both, for amplitude and phase, there is a relationship between standard deviation and frequency; 2) different signals produce different behaviors[3]; 3) amplitude results are very similar for DFT and fitting methods; and 4) phase results of DFT and fitting methods become more similar as frequency increases.

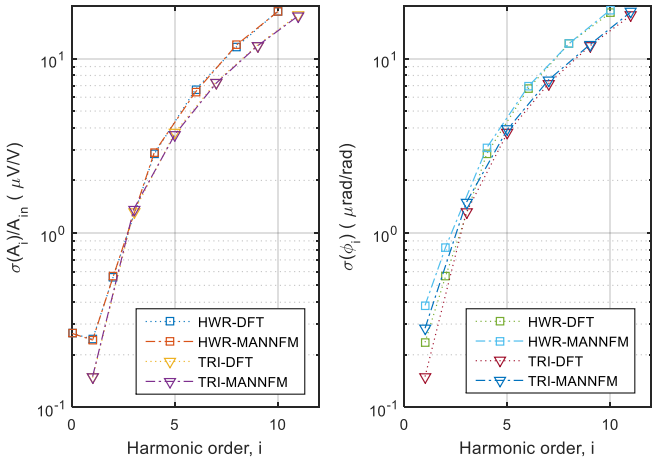

Fig. 4. Standard deviations of amplitude and phase deviations to nominal for HWR and TRI signals for different harmonics - only quantization considered

[3] Only in the case of amplitude considering exclusively jitter, for both signals, very similar behaviors are appreciated. In the rest of cases (included phase deviations considering exclusively jitter) different behaviors are observed.

6.2 Impact of R and N

In order to reduce the number of simulations and taking into considerations sinusoidal results, *R* and *N* effects were studied separately. Firstly, it was confirmed that the results do not depend on the particular value of parameter *R*. That was tested considering points of high number of samples (*N*=15457) from Table 1. Half wave rectified signal was used, with 100 ns of jitter value and 16 bits of quantization. Detailed results are included as tables in Appendix I, while figures 5 and 6 show standard deviations to nominal values, for amplitude (μV/V) and phase (μrad) respectively. *R* values are indicated in labels.

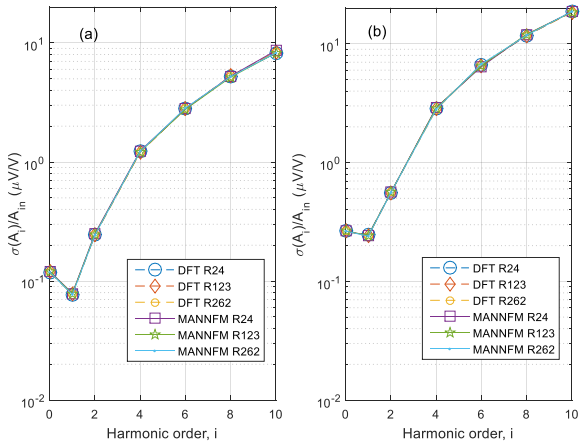

Fig. 5. Standard deviations of amplitude deviations to nominal of the HWR signal harmonics, with 100 ns jitter, 16 bits of quantization, 15457 samples and different *R* values, considering: a) jitter considered, b) only quantization

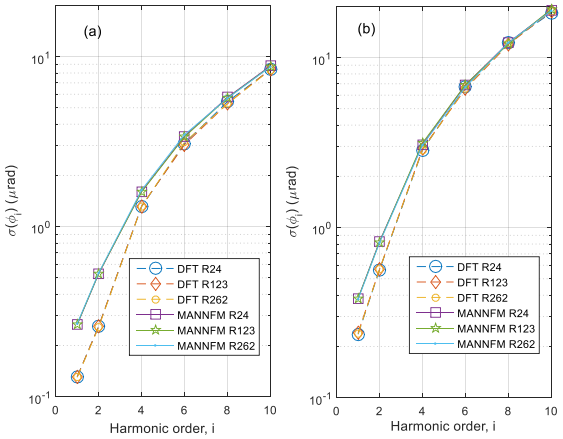

Fig. 6. Standard deviations of phase deviations to nominal of the HWR signal harmonics, with 100 ns jitter, 16 bits of quantization, 15457 samples and different *R* values, considering: a) jitter considered, b) only quantization

From results shown in Fig. 5 and 6 it is clear that, for all methods and all harmonics amplitudes and phases, there is no dependence of standard deviations with the R value. Besides, both figures also confirm conclusions obtained in section 6.1.2.

Consequently, results' dependence with N was tested for just one R value (R=24), considering the last three points from Table 1. Again, half wave rectified signal was used, with 100 ns of jitter value and 16 bits of quantization. Detailed results are included as tables in Appendix II, while Fig. 7 and 8 show standard deviations to nominal values, for amplitude (μV/V) and phase (μrad) respectively. N values are indicated in labels.

Figures 7 and 8 show clearly that, for all methods and all harmonics amplitudes and phases, there is a dependence of the standard deviations with the value of N (as it was concluded in [12] for sinusoidal signals). More precisely, it can be checked that amplitude and phase uncertainties, for both jitter and quantization, are inversely proportional to the factor $\sqrt{N}$, as it is expected for DFT [17] [18]. Finally, conclusions of section 6.1.2 are confirmed again.

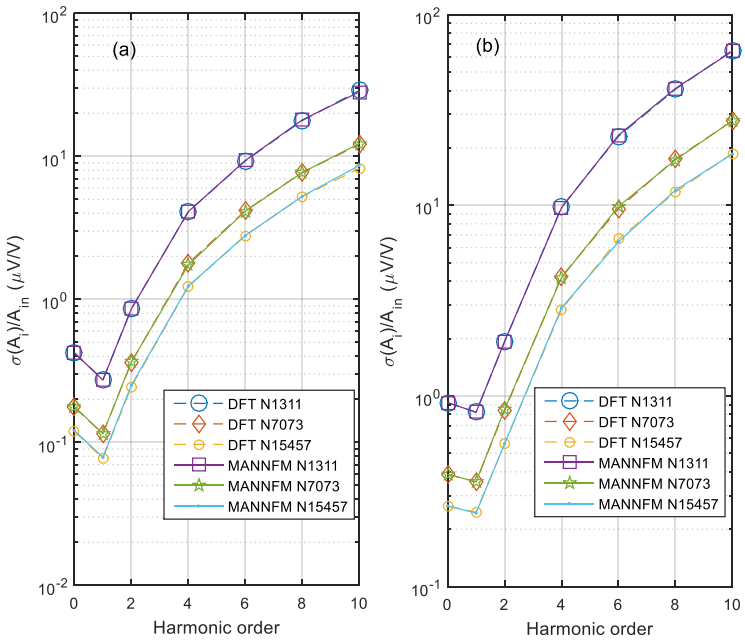

Fig. 7. Standard deviations of amplitude deviations to nominal of the HWR signal harmonics, with 100 ns jitter, 16 bits of quantization, R fixed to 24 and different N values, considering: a) jitter considered, b) only quantization

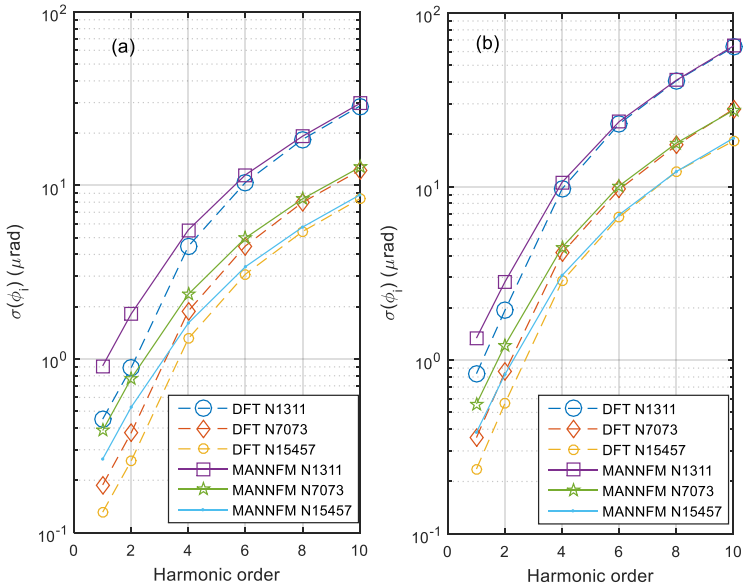

Fig. 8. Standard deviations of phase deviations to nominal of the HWR signal harmonics, with 100 ns jitter, 16 bits of quantization, *R* fixed to 24 and different *N* values, considering: a) jitter considered, b) only quantization

6.3 Impact of jitter and the number of bits

In order to evaluate the effect of jitter and the number of bits on the method behaviour with the minimum number of points, results obtained in [12] were taken into consideration. As it can be seen in [12], for maximum jitter value 3 ps, jitter effect can be discarded for any number of bits. To confirm this conclusion with harmonic content, for maximum jitter 3 ps, a simulation was performed in the point where jitter and quantitation contributions are closer, that is, 15457 samples with 21 bits of resolution (with low ratio, *R*=24). As it can be seen in Table 9, simulation results show that even in this point, jitter effects are three orders of magnitude lower than quantization effects. Consequently, only the maximum jitter value of 100 ns was considered for simulations (*R* was fixed to the low value), so that only 9 points were simulated. Detailed results for DFT and MANNFM are included as tables in Appendix III, while figures 9 to 12 presents these results graphically.

		Amplitude		Phase	
Method	**Harm**	**j**	**q**	**j**	**q**
DFT	**0**	3.61E-06	8.26E-03	--	--
	1	2.36E-06	7.40E-03	3.95E-06	7.76E-03
	2	7.30E-06	1.73E-02	7.60E-06	1.79E-02
	4	3.62E-05	8.86E-02	3.89E-05	9.06E-02
	6	8.46E-05	2.09E-01	9.54E-05	2.05E-01
	8	1.55E-04	3.73E-01	1.59E-04	3.69E-01
	10	2.49E-04	5.99E-01	2.51E-04	5.90E-01
MANNFM	**0**	3.57E-06	8.26E-03	--	--
	1	2.31E-06	7.65E-03	7.82E-06	1.21E-02
	2	7.46E-06	1.79E-02	1.56E-05	2.58E-02
	4	3.58E-05	8.92E-02	4.73E-05	9.51E-02
	6	8.75E-05	1.99E-01	9.81E-05	2.13E-01
	8	1.54E-04	3.73E-01	1.64E-04	3.76E-01
	10	2.53E-04	5.57E-01	2.47E-04	6.01E-01

Table 9. Standard deviation of HWR harmonics deviations to amplitude nominal values (μV/V) and phase nominal values (μrad) for *3 ps* of maximum jitter, *21* bits of resolution and *15457* samples, considering: only jitter (*j*), only quantization (*q*)

For the nine points simulated, figures 9 and 10 show standard deviations to amplitude (μV/V) and phase (μrad) nominal values respectively, considering only jitter. Number of bits values are indicated in labels. Due to space limitations, methods are labelled as D (DFT) and M (MANNFM).

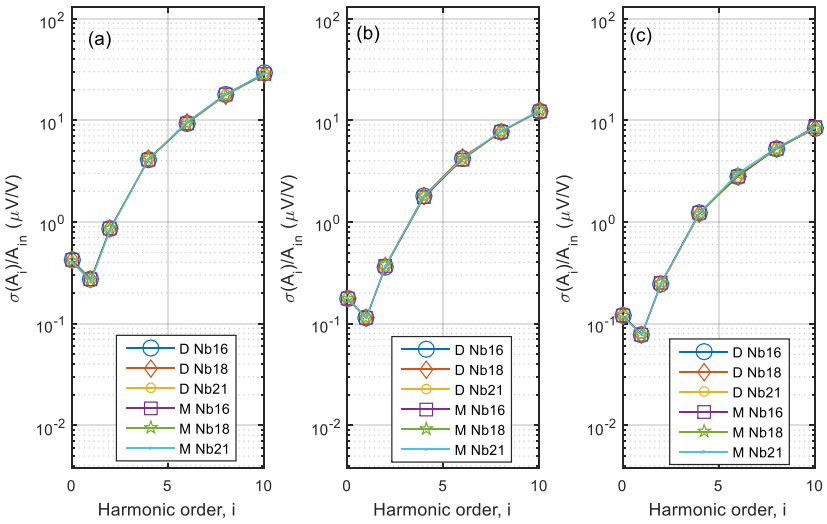

Fig. 9. Standard deviations, considering only jitter, of amplitude deviations to nominal of the HWR signal harmonics, with 100 ns jitter, *R* fixed to 24 and different number of bits values, for *N* values: a) N=1311, b) N=7073, c) N=15457

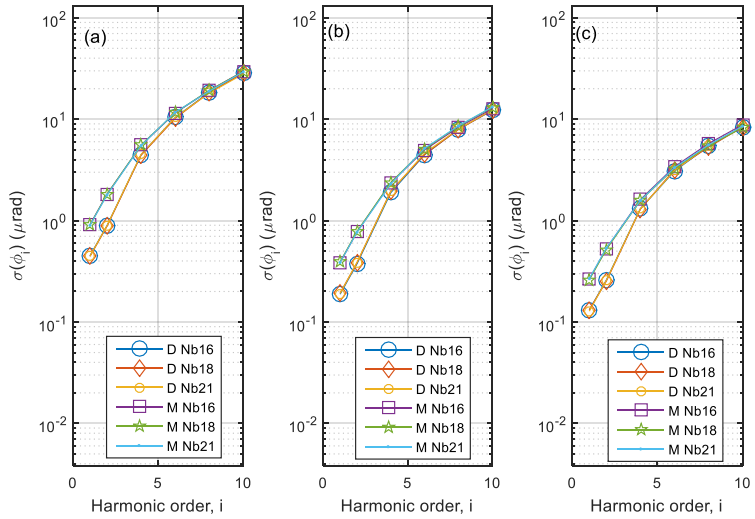

Fig. 10. Standard deviations, considering only jitter, of amplitude deviations to nominal of the HWR signal harmonics, with 100 ns jitter, *R* fixed to 24 and different number of bits values, for *N* values: a) N=1311, b) N=7073, c) N=15457

For the nine points simulated, Fig. 11 and 12 show standard deviations to amplitude (μV/V) and phase (μrad) nominal values respectively, considering only quantization. Number of bits values are indicated in labels. Due to space limitations, methods are labelled as D (DFT) and M (MANNFM).

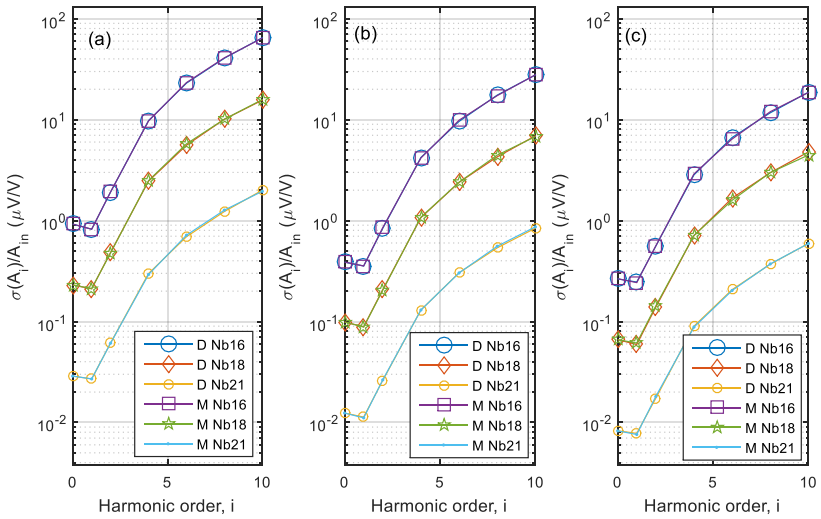

Fig. 11. Standard deviations, considering only quantization, of amplitude deviations to nominal of the HWR signal harmonics, with 100 ns jitter, *R* fixed to 24 and different number of bits values, for *N* values: a) N=1311, b) N=7073, c) N=15457

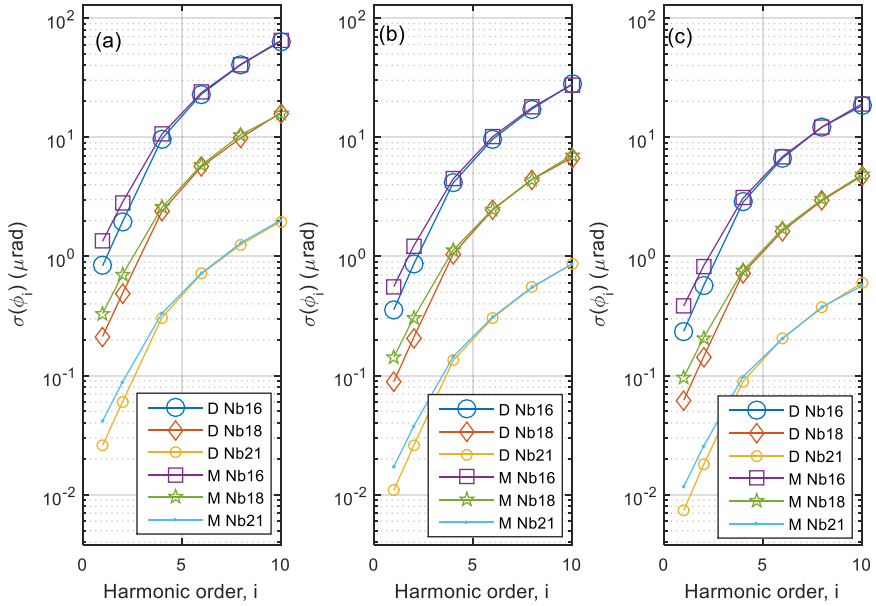

Fig. 12. Standard deviations, considering only quantization, of phase deviations to nominal of the HWR signal harmonics, with 100 ns jitter, *R* fixed to 24 and different number of bits values, for *N* values: a) N=1311, b) N=7073, c) N=15457

Concerning results considering only jitter, it is clear from figures 9 and 10 that there is a dependence only with the number of samples, decreasing amplitude and phase standard deviation as *N* gets higher.

Concerning results considering only quantization, figures 11 and 12 show the expected behaviour respecting resolution for both amplitude and phase standard deviations. The overlap on the ordinates of different *N* value sub-figures shows graphically, as it was introduced in [12], that the increase of standard deviation due to a necessary resolution reduction can be partially compensated increasing the number of samples. From figures it is also clear that not all reductions can be completely compensated[4].

Regarding the contribution of jitter and quantization in the combined uncertainty, it can also be seen from figures 9 to 12, independently of the *N* value, that:

- for 16 bits of resolution, quantization is the most important effect (combined value is slightly higher than the quantization value);

[4] For example, for amplitude standard deviation, supposing a starting point of 21 bits and 1311 samples and a resolution reduction from 21 to 18 bits, it can be mostly compensated if N=15457 is fixed. Nevertheless if, in the same starting point, the reduction is from 21 to 16 bits, the uncertainty obtained with 16 bits at 15457 samples is one order of magnitude higher than the initial one.

- 2) for 18 bits of resolution, although jitter is slightly higher, both effects contribute to combined uncertainty;
- 3) for 21 bits of resolution, jitter becomes one order of magnitude higher than quantization and the combined effect can be approximated just by its contribution.

Finally, figures show clear that both methods behaviour:

- regarding amplitudes, MANNFM and DFT have virtually identical standard deviations;
- regarding phases, DFT have lower standard deviations than MANNFM, although the higher the harmonic, the lower the difference, so that above 5th harmonic values are virtually identical.

7 Conclusions

In this article we have carried out an exhaustive analysis to evaluate the uncertainty of the multiharmonic artificial neural network fitting method, MANNFM, with MCM. The analysis has been performed also as a comparison of MANNFM with the MSFM and DFT methods, in order to establish similarities between methods' behaviours. This analysis was performed for sinusoidal signals in [12] and has been widely extended here for the case of signals with harmonic content.

The signals with harmonic content have been carefully chosen so that results obtained are useful in normal calibrations. Thus, analysis performed for sinusoidal signals and signals with harmonic content (up to 10th harmonic), has provided two principal outcomes: first, a comparison of the three methods, *MANNFM*, *MSFM* and *DFT* in terms of uncertainty; and second, a set of practical standard deviation values of these methods for its use in practical laboratory measurements. Tables with the obtained values have been included in appendixes.

Regarding method comparison, results show that, in both amplitude and phase parameters, deviations to nominal of fitting methods, *MANNFM* and *MSFM*, have virtually identical mean and standard deviations for all the cases and signals studied. This result is the expected one, because both methods solve the same optimization problem in different ways. Compared with DFT, in all simulations performed fitting methods provides similar standard deviation in amplitude but higher in phase. Nevertheless, harmonic tests have shown that the higher the frequency, the more similar the phase standard deviation values are, becoming practically equal from the 5th harmonic. This conclusion is very significant, since it implies that, from the fifth harmonic (where contributions to uncertainty becomes substantial for laboratory measurements), fitting methods and DFT can be considered identical in terms of standard deviations of amplitude and phase, which implies, in fact, that in those situations where synchronous sampling is not possible, spectrum analysis with asynchronous methods can be performed without incurring in uncer-

tainty increases. And, even more, that conclusion implies that fitting methods' uncertainties can be approximated analytically from DFT state of the art [17] [18].

Regarding the set of values obtained - for 95.5% of confidence level (2σ) -, for sinusoidal signals, in the worst case (N= 1311, *Nbits*=16, *Maxjitt*=100 ns), results show uncertainties lower than 1.7 μV and 2.1 μrad for amplitude and phase, respectively. Concerning signals with harmonic content, the study shows a slightly dependence of the results with the signal spectrum. Same test performed for sinusoidal signal has also been carried out for half wave rectified signal and the results have been presented. In the worst case, standard deviations for amplitude reach 140 μV/V, while 157 μrad are obtained for phase both for the 10th harmonic of the half wave rectified signal.

Acknowledgments

This work was partially supported by the Universidad de Malaga - Campus de Excelencia Andalucia-Tech.

References

1. S. Svensson.: "Power Measurement techniques for nonsinusoidal conditions", Doctoral Thesis, Chalmers University of Technology, Sweden (1999)
2. P.S. Wright: "Traceability in power/reactive power measurements and assessment tests for 'IEC555 power analyzers', using the NPL Mk.III digital sampling wattmeter", IEE Colloquium on Low Frequency Power Measurement and Analysis (Digest No. 1994/203), pp. 1/1-1/6 (1994)
3. A. V. Oppenheim and R. W. Schafer, "Discrete-Time Signal Processing". Upper Saddle River, NJ: Prentice-Hall, 1999.
4. U. Pogliano: "Use of integrative analog-to-digital converters for high-precision measurement of electrical power", IEEE Transactions on Instrumentation and Measurement 50(5), 1315–1318 (2001)
5. J. R. Salinas F.G. Lagos, G. Joya and F. Sandoval., "New Spanish electrical power standard," MELECON 2006 - 2006 IEEE Mediterranean Electrotechnical Conference, Malaga, Spain, 2006, pp. 994-997.
6. IEEE standard 1241, 2010, Waveform Measurement and Analysis Technical committee, IEEE Standard for Terminology and Test Methods for Analog-to-Digital Converters (2010)
7. P. M. Ramos and A. Cruz Serra, "Least Squares Multiharmonic Fitting: Convergence Improvements," IEEE Transactions on Instrumentation and Measurement, vol. 56, no. 4, pp. 1412-1418, Aug. 2007.
8. J.R. Salinas, F. García-Lagos, G. Joya, and F. Sandoval," Sine Fitting Multiharmonic Algorithms implemented by Artificial Neural Networks", Neurocomputing, Vol. 72 No.16-18, pp. 3640-3648. 2009.

9. J.R. Salinas, F.G. Lagos, M.L. Romero, G. Joya, F. Raso, M. Neira and F. Sandoval.: "Versatile Digital System for High Accuracy Power Measurements". Conference on Precision Electromagnetic Measurements (CPEM 2006), pp. 98–99, July 2006.
10. J.R. Salinas, J. Díaz de Aguilar, F. García-Lagos, G. Joya, F. Sandoval and M.L. Romero, "Spectrum analysis of asynchronously sampled signals by means of an ANN Method", Conference on Precision Electromagnetic Measurements (CPEM 2014), pp. 422-423, August 2014.
11. J. R. Salinas, F. García-Lagos, J. D. de Aguilar, G. Joya, R. Lapuh and F. Sandoval, "Harmonics and interharmonics spectral analysis by ANN", 2016 Conference on Precision Electromagnetic Measurements (CPEM 2016), Ottawa, Canada, 2016, pp. 1-2.
12. J.R, Salinas, F. García-Lagos, J.D. de Aguilar, G. Joya, F. Sandoval, "Uncertainty Analysis of ANN-Based Spectral Analysis Using Monte Carlo Method". In: Rojas I., Joya G., Catala A. (eds) Advances in Computational Intelligence. IWANN 2017. Lecture Notes in Computer Science, vol. 10305, pp. 269-280, Springer, Cham, 2017.
13. JGCM 100:2008. Evaluation of measurement data –Guide to the expression of uncertainty in measurement.
14. JGCM 101:2008. Evaluation of measurement data – Supplement 1 to the "Guide to the expression of uncertainty in measurement" – Propagation of distributions using a Monte Carlo method.
15. JGCM 102:2011. Evaluation of measurement data – Supplement 2 to the "Guide to the expression of uncertainty in measurement" – Extension to any number of output quantities.
16. M. Šíra and S. Mašláň, "Uncertainty analysis of non-coherent sampling phase meter with four parameter sine wave fitting by means of Monte Carlo", 29th Conference on Precision Electromagnetic Measurements (CPEM 2014), Rio de Janeiro, pp. 334-335, 2014.
17. M. F. Wadgy, "Effects of ADC quantization errors on some periodic signal measurements", IEEE Trans. Instr. Meas., Vol. 36, No.4, pp. 983-988, Dec. 1987.
18. M. F. Wagdy and S. S. Awad, "Effect of sampling jitter on some sine wave measurements," IEEE Transactions on Instrumentation and Measurement, vol. 39, no. 1, pp. 86-89, Feb. 1990.
19. V. K. Jain, W. L. Collins and D. C. Davis, "High-Accuracy Analog Measurements via Interpolated FFT", IEEE Transactions on Instrumentation and Measurement, vol. 28, no. 2, pp. 113-122, June 1979.
20. EN 50470-3:2006. Electricity metering equipment (a.c.) -- Part 3: Particular requirements - Static meters for active energy (class indexes A, B and C).

Conflict of Interest

The authors declare that they have no conflict of interest.

Appendix I

Tables I.1 and I.2 show standard deviation results obtained for amplitude and phase of half wave rectified harmonics for the case of a jitter value of 100 ns and 16 bits of quantization, 15457 samples and different R values. In order to unify data as much as possible, both tables simultaneously present values obtained considering only jitter (j) and only quantization (q).

		j			q		
		R			*R*		
Method	**Harm**	**24**	**123**	**262**	**24**	**123**	**262**
DFT	**0**	1.19E-01	1.20E-01	1.19E-01	2.65E-01	2.65E-01	2.65E-01
	1	7.72E-02	7.83E-02	7.73E-02	2.46E-01	2.43E-01	2.40E-01
	2	2.45E-01	2.44E-01	2.44E-01	5.59E-01	5.59E-01	5.63E-01
	4	1.23E+00	1.21E+00	1.21E+00	2.84E+00	2.88E+00	2.79E+00
	6	2.79E+00	2.79E+00	2.82E+00	6.66E+00	6.55E+00	6.70E+00
	8	5.24E+00	5.28E+00	5.24E+00	1.17E+01	1.18E+01	1.18E+01
	10	8.23E+00	8.39E+00	8.40E+00	1.87E+01	1.84E+01	1.85E+01
MANNFM	**0**	1.21E-01	1.20E-01	1.19E-01	2.65E-01	2.65E-01	2.65E-01
	1	7.88E-02	7.84E-02	7.71E-02	2.43E-01	2.44E-01	2.40E-01
	2	2.51E-01	2.47E-01	2.44E-01	5.62E-01	5.61E-01	5.60E-01
	4	1.24E+00	1.22E+00	1.23E+00	2.90E+00	2.88E+00	2.81E+00
	6	2.80E+00	2.77E+00	2.84E+00	6.43E+00	6.55E+00	6.76E+00
	8	5.26E+00	5.16E+00	5.22E+00	1.20E+01	1.20E+01	1.18E+01
	10	8.63E+00	8.24E+00	8.25E+00	1.86E+01	1.85E+01	1.87E+01

Table I.1. Standard deviation of HWR harmonics deviations to amplitude nominal values (μV/V) in high number of samples points of Table 1, considering only: jitter (*j*), quantization (*q*)

		j			q		
		R			*R*		
Method	**Harm**	**24**	**123**	**262**	**24**	**123**	**262**
DFT	**1**	1.31E-01	1.31E-01	1.30E-01	2.36E-01	2.41E-01	2.37E-01
	2	2.59E-01	2.59E-01	2.56E-01	5.65E-01	5.68E-01	5.70E-01
	4	1.31E+00	1.32E+00	1.31E+00	2.85E+00	2.90E+00	2.86E+00
	6	3.08E+00	3.03E+00	3.13E+00	6.69E+00	6.53E+00	6.59E+00
	8	5.42E+00	5.28E+00	5.27E+00	1.22E+01	1.19E+01	1.21E+01
	10	8.36E+00	8.42E+00	8.34E+00	1.83E+01	1.87E+01	1.87E+01
MANNFM	**1**	2.65E-01	2.66E-01	2.69E-01	3.84E-01	3.84E-01	3.79E-01
	2	5.28E-01	5.30E-01	5.34E-01	8.29E-01	8.21E-01	8.15E-01
	4	1.61E+00	1.60E+00	1.64E+00	3.08E+00	3.14E+00	3.05E+00
	6	3.40E+00	3.37E+00	3.47E+00	6.89E+00	6.91E+00	6.69E+00
	8	5.75E+00	5.70E+00	5.68E+00	1.22E+01	1.20E+01	1.22E+01
	10	8.80E+00	8.73E+00	8.70E+00	1.90E+01	1.92E+01	1.88E+01

Table I.2. Standard deviation of HWR harmonics deviations to phase nominal values (μrad) in high number of samples points of Table 1, considering only: jitter (*j*), quantization (*q*)

Appendix II

Tables II.1 and II.2 show standard deviation results obtained for amplitude and phase of half wave rectified harmonics for the case of a jitter value of 100 ns and 16 bits of quantization, R fixed to 24 and different N values. In order to unify data as much as possible, both tables simultaneously present values obtained considering only jitter (j) and only quantization (q).

		j			q		
		N			N		
Method	Harm	1311	7073	15457	1311	7073	15457
DFT	0	4.24E-01	1.76E-01	1.19E-01	9.23E-01	3.88E-01	2.65E-01
	1	2.74E-01	1.15E-01	7.72E-02	8.21E-01	3.55E-01	2.46E-01
	2	8.59E-01	3.63E-01	2.45E-01	1.92E+00	8.38E-01	5.59E-01
	4	4.11E+00	1.79E+00	1.23E+00	9.79E+00	4.22E+00	2.84E+00
	6	9.29E+00	4.16E+00	2.79E+00	2.30E+01	9.61E+00	6.66E+00
	8	1.78E+01	7.73E+00	5.24E+00	4.06E+01	1.75E+01	1.17E+01
	10	2.89E+01	1.21E+01	8.23E+00	6.49E+01	2.77E+01	1.87E+01
MANNFM	0	4.23E-01	1.78E-01	1.21E-01	9.23E-01	3.88E-01	2.65E-01
	1	2.73E-01	1.15E-01	7.88E-02	8.22E-01	3.55E-01	2.43E-01
	2	8.58E-01	3.65E-01	2.51E-01	1.93E+00	8.51E-01	5.62E-01
	4	4.11E+00	1.74E+00	1.24E+00	9.71E+00	4.17E+00	2.90E+00
	6	9.36E+00	4.14E+00	2.80E+00	2.33E+01	9.87E+00	6.43E+00
	8	1.80E+01	7.72E+00	5.26E+00	4.10E+01	1.73E+01	1.20E+01
	10	2.82E+01	1.23E+01	8.63E+00	6.43E+01	2.78E+01	1.86E+01

Table II.1. Standard deviation of HWR harmonics deviations to amplitude nominal values (μV/V) in last three points of Table 1, considering: only jitter (j), only quantization (q)

		j			q		
		N			N		
Method	Harm	1311	7073	15457	1311	7073	15457
DFT	1	4.50E-01	1.88E-01	1.31E-01	8.36E-01	3.58E-01	2.36E-01
	2	8.91E-01	3.76E-01	2.59E-01	1.94E+00	8.55E-01	5.65E-01
	4	4.46E+00	1.89E+00	1.31E+00	9.71E+00	4.14E+00	2.85E+00
	6	1.04E+01	4.48E+00	3.08E+00	2.30E+01	9.63E+00	6.69E+00
	8	1.84E+01	7.99E+00	5.42E+00	4.07E+01	1.73E+01	1.22E+01
	10	2.86E+01	1.22E+01	8.36E+00	6.36E+01	2.79E+01	1.83E+01
MANNFM	1	9.12E-01	3.87E-01	2.65E-01	1.34E+00	5.59E-01	3.84E-01
	2	1.82E+00	7.72E-01	5.28E-01	2.83E+00	1.22E+00	8.29E-01
	4	5.54E+00	2.36E+00	1.61E+00	1.06E+01	4.47E+00	3.08E+00
	6	1.15E+01	4.98E+00	3.40E+00	2.37E+01	1.01E+01	6.89E+00
	8	1.92E+01	8.36E+00	5.75E+00	4.10E+01	1.78E+01	1.22E+01
	10	2.96E+01	1.27E+01	8.80E+00	6.46E+01	2.75E+01	1.90E+01

Table II.2. Standard deviation of HWR harmonics deviations to phase nominal values (μrad) in last three points of Table 1, considering: only jitter (j), only quantization (q)

Appendix III

Tables III.1 and III.2 show standard deviation results obtained for amplitude and phase of half wave rectified harmonics for the case of a jitter value of 100 ns, *R* fixed to 24, different *N* values and different number of bits. Due to the amount of data to be included values obtained considering only jitter (*j*) are presented.

Tables III.3 and III.4 show standard deviation results obtained for amplitude and phase of half wave rectified harmonics for the case of a jitter value of 100 ns, *R* fixed to 24, different *N* values and different number of bits. Due to the amount of data to be included both tables present only values obtained considering only jitter (*q*).

		N								
		1311			7073			15457		
		Nbits			Nbits			Nbits		
Method	Harm	16	18	21	16	18	21	16	18	21
DFT	0	4.24E-01	4.19E-01	4.01E-01	1.76E-01	1.75E-01	1.80E-01	1.19E-01	1.20E-01	1.21E-01
	1	2.74E-01	2.72E-01	2.62E-01	1.15E-01	1.13E-01	1.15E-01	7.72E-02	7.87E-02	7.90E-02
	2	8.59E-01	8.61E-01	8.33E-01	3.63E-01	3.70E-01	3.66E-01	2.45E-01	2.43E-01	2.42E-01
	4	4.11E+00	4.16E+00	4.17E+00	1.79E+00	1.81E+00	1.78E+00	1.23E+00	1.21E+00	1.21E+00
	6	9.29E+00	9.46E+00	9.63E+00	4.16E+00	4.35E+00	4.06E+00	2.79E+00	2.82E+00	2.80E+00
	8	1.78E+01	1.76E+01	1.80E+01	7.73E+00	7.63E+00	7.59E+00	5.24E+00	5.18E+00	5.29E+00
	10	2.89E+01	2.82E+01	2.82E+01	1.21E+01	1.24E+01	1.21E+01	8.23E+00	8.29E+00	8.33E+00
MANNFM	0	4.23E-01	4.15E-01	4.02E-01	1.78E-01	1.76E-01	1.79E-01	1.21E-01	1.19E-01	1.18E-01
	1	2.73E-01	2.73E-01	2.63E-01	1.15E-01	1.13E-01	1.15E-01	7.88E-02	7.71E-02	7.82E-02
	2	8.58E-01	8.57E-01	8.31E-01	3.65E-01	3.76E-01	3.66E-01	2.51E-01	2.49E-01	2.47E-01
	4	4.11E+00	4.19E+00	4.14E+00	1.74E+00	1.81E+00	1.78E+00	1.24E+00	1.19E+00	1.23E+00
	6	9.36E+00	9.24E+00	9.56E+00	4.14E+00	4.15E+00	4.23E+00	2.80E+00	2.92E+00	3.02E+00
	8	1.80E+01	1.75E+01	1.79E+01	7.72E+00	7.74E+00	7.82E+00	5.26E+00	5.14E+00	5.36E+00
	10	2.82E+01	2.77E+01	2.87E+01	1.23E+01	1.24E+01	1.24E+01	8.63E+00	8.39E+00	8.49E+00

Table III.1. Standard deviation of HWR harmonics deviations to amplitude nominal values (μV/V) for *Maxjit*=100 ns, *Nbits* and *N* values simulated, considering only jitter (*j*)

		N								
		1311			7073			15457		
		Nbits			Nbits			Nbits		
Method	Harm	16	18	21	16	18	21	16	18	21
DFT	1	4.50E-01	4.44E-01	4.46E-01	1.88E-01	1.93E-01	1.91E-01	1.31E-01	1.32E-01	1.28E-01
	2	8.91E-01	8.82E-01	8.93E-01	3.76E-01	3.84E-01	3.88E-01	2.59E-01	2.53E-01	2.57E-01
	4	4.46E+00	4.42E+00	4.50E+00	1.89E+00	1.96E+00	1.94E+00	1.31E+00	1.30E+00	1.31E+00
	6	1.04E+01	1.02E+01	1.04E+01	4.48E+00	4.50E+00	4.64E+00	3.08E+00	3.18E+00	3.11E+00
	8	1.84E+01	1.83E+01	1.81E+01	7.99E+00	7.92E+00	8.01E+00	5.42E+00	5.30E+00	5.50E+00
	10	2.86E+01	2.85E+01	2.79E+01	1.22E+01	1.23E+01	1.24E+01	8.36E+00	8.38E+00	8.39E+00
MANNFM	1	9.12E-01	9.05E-01	8.98E-01	3.87E-01	3.92E-01	3.86E-01	2.65E-01	2.61E-01	2.68E-01
	2	1.82E+00	1.82E+00	1.79E+00	7.72E-01	7.82E-01	7.69E-01	5.28E-01	5.19E-01	5.36E-01
	4	5.54E+00	5.56E+00	5.50E+00	2.36E+00	2.38E+00	2.31E+00	1.61E+00	1.58E+00	1.58E+00
	6	1.15E+01	1.16E+01	1.17E+01	4.98E+00	5.09E+00	5.18E+00	3.40E+00	3.27E+00	3.33E+00
	8	1.92E+01	1.92E+01	1.89E+01	8.36E+00	8.56E+00	8.59E+00	5.75E+00	5.46E+00	5.57E+00
	10	2.96E+01	2.95E+01	2.93E+01	1.27E+01	1.31E+01	1.32E+01	8.80E+00	8.25E+00	8.55E+00

Table III.2. Standard deviation of HWR harmonics deviations to phase nominal values (μrad) for *Maxjit*=100 ns, *Nbits* and *N* values simulated, considering only jitter (*j*)

		N								
		1311			7073			15457		
		Nbits			Nbits			Nbits		
Method	Harm	16	18	21	16	18	21	16	18	21
DFT	0	9.23E-01	2.30E-01	2.88E-02	3.88E-01	9.90E-02	1.24E-02	2.65E-01	6.61E-02	8.26E-03
	1	8.21E-01	2.11E-01	2.70E-02	3.55E-01	8.86E-02	1.13E-02	2.46E-01	5.92E-02	7.80E-03
	2	1.92E+00	4.85E-01	6.14E-02	8.38E-01	2.07E-01	2.61E-02	5.59E-01	1.39E-01	1.74E-02
	4	9.79E+00	2.46E+00	2.99E-01	4.22E+00	1.07E+00	1.30E-01	2.84E+00	7.09E-01	8.99E-02
	6	2.30E+01	5.58E+00	6.92E-01	9.61E+00	2.39E+00	3.04E-01	6.66E+00	1.67E+00	2.07E-01
	8	4.06E+01	1.01E+01	1.23E+00	1.75E+01	4.28E+00	5.37E-01	1.17E+01	2.98E+00	3.70E-01
	10	6.49E+01	1.56E+01	2.00E+00	2.77E+01	6.91E+00	8.41E-01	1.87E+01	4.79E+00	5.93E-01
MANNFM	0	9.23E-01	2.30E-01	2.88E-02	3.88E-01	9.90E-02	1.24E-02	2.65E-01	6.61E-02	8.26E-03
	1	8.22E-01	2.12E-01	2.70E-02	3.55E-01	8.83E-02	1.11E-02	2.43E-01	6.12E-02	7.60E-03
	2	1.93E+00	4.79E-01	6.11E-02	8.51E-01	2.04E-01	2.64E-02	5.62E-01	1.43E-01	1.81E-02
	4	9.71E+00	2.49E+00	2.92E-01	4.17E+00	1.08E+00	1.30E-01	2.90E+00	7.13E-01	8.80E-02
	6	2.33E+01	5.76E+00	7.17E-01	9.87E+00	2.40E+00	3.03E-01	6.43E+00	1.59E+00	2.03E-01
	8	4.10E+01	1.01E+01	1.27E+00	1.73E+01	4.45E+00	5.57E-01	1.20E+01	2.99E+00	3.72E-01
	10	6.43E+01	1.58E+01	1.95E+00	2.78E+01	6.79E+00	8.67E-01	1.86E+01	4.46E+00	5.93E-01

Table III.3. Standard deviation of HWR harmonics deviations to amplitude nominal values (μV/V) for *Maxjit*=100 ns, *Nbits* and *N* values simulated, considering only quantization (*q*)

		N								
		1311			7073			15457		
		Nbits			Nbits			Nbits		
Method	Harm	16	18	21	16	18	21	16	18	21
DFT	1	8.36E-01	2.13E-01	2.60E-02	3.58E-01	8.88E-02	1.09E-02	2.36E-01	6.21E-02	7.37E-03
	2	1.94E+00	4.86E-01	5.97E-02	8.55E-01	2.08E-01	2.58E-02	5.65E-01	1.43E-01	1.78E-02
	4	9.71E+00	2.39E+00	3.07E-01	4.14E+00	1.05E+00	1.34E-01	2.85E+00	7.25E-01	8.94E-02
	6	2.30E+01	5.67E+00	7.15E-01	9.63E+00	2.46E+00	3.04E-01	6.69E+00	1.64E+00	2.06E-01
	8	4.07E+01	9.90E+00	1.26E+00	1.73E+01	4.43E+00	5.51E-01	1.22E+01	2.95E+00	3.72E-01
	10	6.36E+01	1.60E+01	1.96E+00	2.79E+01	6.73E+00	8.64E-01	1.83E+01	4.72E+00	5.96E-01
MANNFM	1	1.34E+00	3.32E-01	4.16E-02	5.59E-01	1.43E-01	1.72E-02	3.84E-01	9.68E-02	1.17E-02
	2	2.83E+00	7.00E-01	8.78E-02	1.22E+00	3.05E-01	3.75E-02	8.29E-01	2.07E-01	2.55E-02
	4	1.06E+01	2.57E+00	3.33E-01	4.47E+00	1.13E+00	1.44E-01	3.08E+00	7.61E-01	9.80E-02
	6	2.37E+01	5.84E+00	7.24E-01	1.01E+01	2.49E+00	3.11E-01	6.89E+00	1.70E+00	2.05E-01
	8	4.10E+01	1.05E+01	1.30E+00	1.78E+01	4.44E+00	5.54E-01	1.22E+01	3.01E+00	3.77E-01
	10	6.46E+01	1.57E+01	2.01E+00	2.75E+01	7.05E+00	8.60E-01	1.90E+01	4.81E+00	5.65E-01

Table III.4. Standard deviation of HWR harmonics deviations to phase nominal values (μrad) for *Maxjit*=100 ns, *Nbits* and *N* values simulated, considering only quantization (*q*)